Journal of Fluorescence (2019) 29:319–333
https://doi.org/10.1007/s10895-018-02341-5

FLUORESCENCE NEWS ARTICLE

Template Synthesis, Spectral, Thermal and Glucose Sensing of Pr^{3+} Complexes of Metformin Schiff-Bases

Marwa Mahmoud[1] · Enas Abdel-Salam[2] · Mahmoud Abou-Elmagd[3] · Shehab Sallam[2]

Received: 20 October 2018 / Accepted: 26 December 2018 / Published online: 16 January 2019

Abstract

Schiff-bases of metformin with each of salicylaldehyde (HL^1); 2,3-dihydroxybenzaldehyde (H_2L^2); 2,4-dihydroxybenzaldehyde (H_2L^3); 2,5-dihydroxybenzaldehyde (H_2L^4); 3,4-dihydroxybenzaldehyde (H_2L^5) and 2-hydroxynaphthaldehyde (HL^6) and their complexes with Pr(III) were synthesized by template reaction. The complexes were characterized through elemental analysis, conductivity and magnetic moment measurements, IR, UV-Vis., fluorescence, GC-MS and XRD spectroscopy. The complexes exhibit a series of characteristic emission bands for Pr^{3+} ion in the 481-472 and 590-580 nm range with a 318-332 nm excitation source. The complexes have eight coordinated structure with the formulae $[PrL^{1\text{-}4,6}(NO_3)_2(H_2O)_3].nH_2O$ where n = 1, 1½, 3, 4, 4 and $[PrL^5(NO_3)(H_2O)_5].2H_2O$. The suggested stereochemistry was confirmed using TGA, DTG and DTA analysis and a mechanism for thermal decomposition was proposed. Coates-Redfern equation was used to calculate kinetic and thermodynamic parameters of the main decomposition step. The utility of the complexes towards the detection of glucose at physiologically relevant pH in phosphate buffer using UV-Vis and fluorescence spectroscopy as well as viscosity measurements are tried where the association constants were calculated.

Keywords Metformin Schiff-bases · Pr(III) complexes · Spectral and thermal properties · Glucose sensing

Introduction

Metformin hydrochloride (MF.HCl; N,N-dimethyl biguanide) is an oral hypoglycemic agent which is commonly prescribed for the treatment of DM type II [1]. There is much interest in MF ligand and its transition metal complexes which are cationic in nature [2–8]. Regarding the potential functions of Schiff-bases, Gao [9] has studied the antimicrobial activity of copper(II) complex derived from the condensation of MF with 2-pyridinecarbaldehyde. In addition, Ni(II) complexes with ligands that resulted in condensation of MF and pentane-2,4-dione were synthesized and characterized [10]. Recently, Cr(III) and VO^{2+} complexes of MF Schiff-bases with each of hydroxy- and dihydroxybenzaldehyde were synthesized by template reaction and found to have antidiabetic activity [11, 12]. On the other hand, Cu(II) complexes with the same Schiff-bases have shown toxicity to alloxane induced-diabetic mice [13].

In the last decades, lanthanide complexes attracted increasing interest in coordination and bioinorganic chemistry due to their interesting structures, and also for their photo-physical, magnetic and biological properties. Due to their special electronic configuration, a variety of lanthanide complexes have been proven to be very good antibacterial, anti-inflammatory, antiviral, anticoagulant and antitumor agents [14–19]. Among them, some of those containing Gd(III) are widely used in biomedical analysis as magnetic resonance imaging (MRI) contrast agents both for its high paramagnetism and favorable properties in terms of electronic relaxation [20].

Due to the biological relevance of lanthanide elements and the biological activity of MF, a series of praseodymium complexes with Schiff-bases of MF with salicylaldehyde (HL^1); 2,3-dihydroxybenzaldehyde (H_2L^2); 2,4-dihydroxybenzaldehyde

Electronic supplementary material The online version of this article (https://doi.org/10.1007/s10895-018-02341-5) contains supplementary material, which is available to authorized users.

✉ Shehab Sallam
shehabsallam@yahoo.com

[1] Department of Science and Mathematics Engineering, Faculty of Petroleum and Mining Engineering, Suez University, Suez, Egypt

[2] Department of Chemistry, Faculty of Science, Suez Canal University, Ismailia, Egypt

[3] Holding Company for Water & Wastewater, Ismailia, Egypt

(H_2L^3); 2,5-dihydroxybenzaldehyde (H_2L^4); 3,4-dihydroxybenzaldehyde (H_2L^5); and 2-hydroxynaphthaldehyde (HL^6) were synthesized by template reaction. The resulting complexes were characterized using elemental analysis, conductivity measurements, magnetic moment values, spectral analysis (UV–Vis, fluorescence, IR, GC-MS, XRD), and TG, DTG and DTA. Also, we describe the utility of the Pr complexes towards the detection of glucose at physiologically relevant pH in phosphate buffer solution using UV-Vis and fluorescence spectra as well as viscosity measurements.

Experimental

Materials

All chemicals used in this study were of A.R. or equivalent grade and were used without further purification. Salicylaldehyde, 2,3-dihydroxybenzaldehyde, 2,4-dihydroxybenzaldehyde, 2,5-dihydroxybenzaldehyde, 3,4-dihydroxybenzaldehyde and 2-hydroxynaphthaldehyde (Koch-light laboratories) were used as such. Metformin–HCl was purchased from El-Nasr Company for Pharmaceutical Chemicals, Cairo, Egypt. $Pr(NO_3)_3.6H_2O$ was obtained from Aldrich Chemical Company. Glucose was supplied by Sigma-Aldrich, St. Louis, Missouri, USA.

Synthesis of the Schiff-Bases

The Schiff-bases have been prepared by addition of methanolic MF solution to a methanolic solution of the aldehyde in 1:1 mol ratio in basic medium [11]. The mixture was refluxed with continuous stirring over water bath for 2 h. The solution turned to yellow color indicating the formation of the Schiff-base. Only, HL^1 Schiff-base was isolated in the solid state, dried under vacuum and recrystallized from methanol (m.p. 195 °C). We followed the same method in preparation of the other Schiff-bases with different aldehydes but trials to obtain the solid compounds were unsuccessful. Accordingly, the Schiff-bases were obtained dissolved in methanol solution and used further for template synthesis of the complexes.

Template Synthesis of the Complexes

All the complexes were prepared according to the following procedure. Solution of $Pr(NO_3)_3.6H_2O$ (1 mmol, 0.435 g) in 10 mL of methanol was added dropwise to methanolic solution of the Schiff-base (1 mmol) prepared in the previous step. The mixture was refluxed on water bath for 2 h with stirring during which a deep green to brown solution is formed (pH = 4–4.5), after which NH_4OH is added dropwise tell the complex is precipitated (pH = 6–7). Stirring is continued for another 1 h at room temperature, the complex is filtered, washed thoroughly with water and hot methanol and dried under vacuum.

Physical Measurements

C, H, and N were estimated using a Heraus CHN-rapid analyzer. The IR spectra were recorded (KBr disc) in the 400–4000 cm^{-1} range on Bruker Vector-22 spectrometer. The electronic absorption spectra were obtained by 10^{-3} M DMSO solution in 1 cm quartz cell using Shimadzu UV-1800 double beam photometric system. Fluorescence spectra were performed on JASCO FP-6300 spectrofluorometer using 1 cm quartz cell type 111-QS with a 150 W xenon lamp for excitation (slit width 5 nm). X-ray powder diffraction was performed using a Brucker Axs-D8 advance diffractometer with Cu-Kα radiation. GC-MS spectra were obtained using Shimadzu Qp-2010 Plus with EI ionization mode and electron voltage 70 eV. Magnetic susceptibility measurements were carried out using the modified Gouy method [21] on MSB-MK1 balance at room temperature using mercury(II)tetrathiocyanatecobaltate(II) as a standard. The effective magnetic moment, μ_{eff},per metal atom was calculated from the expression $\mu_{eff} = 2.83\sqrt{\chi.T}$ B.M., where χ is the molar susceptibility corrected using Pascal's constant for the diamagnetism of all atoms in the complexes. TGA, DTG and DTA were recorded on Shimadzu H-60 thermal analyzer under a dynamic flow of nitrogen (30 ml/min.) and heating rate 10 °C/min. from ambient temperature to 750 or 1000 °C. Electrical conductivity measurements were carried out at room temperature on freshly prepared 10^{-3} M DMF solutions using WTW conductivity meter fitted with L100 conductivity cell. Metal content was obtained by EDTA titration using xylenol orange as indicator using acetate buffer.

Results and Discussion

The Schiff-bases were prepared by addition of methanolic MF solution to a methanolic solution of the aldehyde in 1:1 mol ratio [11] in basic medium (drops of NaOH, CH_3COONa or NH_4OH). The mixture was refluxed with continuous stirring over water bath for 2 h. The solution was turned to yellow color indicating the formation of the Schiff-base. The purity was checked by TLC using methanol-chloroform solvent mixture (1:10 *v*/v). HL^1 Schiff-base was characterized using C, H, N analysis, ^1H NMR, UV–Vis and GC-MS spectra as well as TGA, DTG and DTA analysis [11]. Its structure is shown in Structure 1.

Praseodymium(III) Complexes

Pr^{3+} complexes with Schiff-bases of HL^1, H_2L^2, H_2L^3, H_2L^4, H_2L^5 and HL^6 were synthesized by template reaction of $Pr(NO_3)_3.6H_2O$ with metformin Schiff-bases in methanol under reflux. The physical and analytical data of the complexes

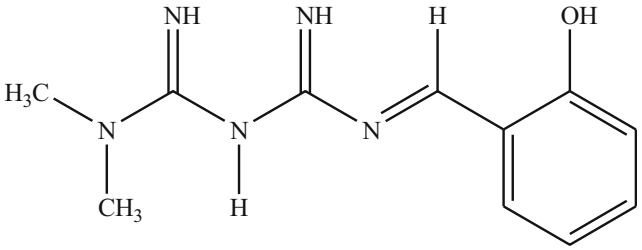

Structure 1 HL^1 Schiff-base

are summarized in Table 1. Results of elemental analysis of the Pr(III) complexes suggest the following molecular formulas: $[PrL^{1-4,6}(NO_3)_2(H_2O)_3].nH_2O$ where $n = 1, 1½, 3, 4, 4$ and $[PrL^5(NO_3)(H_2O)_5].2H_2O$. The complexes were found to be air stable and they decomposed over 380 °C (Table 1). They are insoluble in water and most organic solvents but soluble in Lewis bases such as DMF and DMSO. The molar conductance values for 10^{-3} M DMF solutions of the prepared complexes at 25 °C are in the range of 4.2–18.6 $\Omega^{-1}cm^2mol^{-1}$ supporting the nonelectrolytic character of these complexes [22]. It shows that the anion is coordinated rather than the ionic association to the Pr(III) cation during complex formation.

Although the newly synthesized metal complexes were soluble in some polar organic solvents like DMSO and DMF, attempts to get crystals suitable for single-crystal studies were not obtained. The X-ray powder diffraction patterns for the complexes were scanned in the $5\text{-}75^0$ at $\lambda =$ 1.540598 Å and are shown in Fig. 1. From the patterns, it is evident that the complexes are amorphous.

IR Spectra

The assignment of the IR bands of the praseodymium complexes have been made by comparing with the bands of HL^1 ligand and structurally similar molecules (Table 2, Figs. S1 and S2 in supplementary file). The major IR spectral features of the presented complexes indicate some characteristics bands of biguanide and Schiff- base moieties. The strong broad band ascribed to υ(OH) of the Schiff-base at 3456 cm^{-1} [11] disappeared in the spectra of praseodymium complexes which accounts for the deprotonation and coordination of the OH group. The hydrated complexes have OH-stretching frequencies as a medium broad band in the 3629-3510 and 3440-3406 cm^{-1} regions. IR spectra of all the complexes except $[PrL^5(NO_3)(H_2O)_5].2H_2O$ showed broad intense bands in the range 3218-3200 cm^{-1} assignable to the stretching vibration of the N–H group. These bands were observed in the spectra of some complexes with biguanide Schiff-bases [9–13].The observed strong split bands in the 1645-1604 and 1604-1587 cm^{-1} ranges can be attributed to υ(C=N) frequency [23]. A band manifested in the 1552-1531 cm^{-1} interval has been assigned to N–C–N stretching. The complexes showed bands in the 1456-1405 and 1364-1306 cm^{-1} regions due to υ(N=O) (υ_5) and $\upsilon_{as}(NO_2)$ (υ_1) of the coordinated nitrate. The $\upsilon_s(NO_2)$ (υ_2) was detected at 1041-1030 cm^{-1}. The separation $\Delta\upsilon = \upsilon_5 - \upsilon_1$ has been used to differentiation between mono, bidentate chelating nitrates and bridging mode. The magnitude of Δυ (Table 2) is indicative of a monodentate nitrate (92-125 cm^{-1}) [24]. The band assignable to υ(C–O) was recorded as a medium band in the 1224-1184 cm^{-1} region confirming deprotonation and coordination of the phenolic oxygen to the praseodymium ion. Two other non-ligand bands are also observed, medium band in the range of 596-466 cm^{-1} which may be attributed to υ(Pr–O) and the other around 521-427 cm^{-1} which may be assigned to υ(Pr–N) vibrations. The band υ(Pr–O) are usually broad, stronger and occurs

Table 1 Analytical data and conductivity measurements of the Pr^{3+} complexes of the metformin Schiff-bases

Compound	Mol.wt.	Formula m/z	Yield %	Color	Decomp. point (°C)	Elemental analysis Found Calcd.%				Ω^*_M DMF
						C	H	N	Pr	
$[PrL^1(NO_3)_2(H_2O)_3].H_2O$	569.11	569.1	55	Dark green	>380	23.0 23.2	3.4 3.8	17.5 17.2	24.1 24.7	18.6
$[PrL^2(NO_3)_2(H_2O)_3].1½H_2O$	594.11	593.2	60	Army green	>380	22.5 22.2	3.2 3.5	16.5 16.4	23.9 23.7	8.1
$[PrL^3(NO_3)_2(H_2O)_3].3H_2O$	621.11	622.2	45	Dark brown	>380	21.1 21.2	4.4 4.1	15.1 15.5	22.5 22.6	5.5
$[PrL^4(NO_3)_2(H_2O)_3].4H_2O$	639.11	638.1	47	Black	>380	20.3 20.6	4.5 4.3	15.6 15.3	22.3 22.0	4.2
$[PrL^5(NO_3)(H_2O)_5].2H_2O$	576.13	577.2	40	Grey	>380	23.1 22.9	4.4 4.6	14.1 14.5	24.0 24.4	4.8
$[PrL^6(NO_3)_2(H_2O)_3].4H_2O$	673.15	672.2	55	Brown	>380	19.2 19.6	4.5 4.1	14.1 14.5	20.4 20.9	5.9

*Conductance of 10^{-3} M ($ohm^{-1}\,cm^2\,mol^{-1}$)

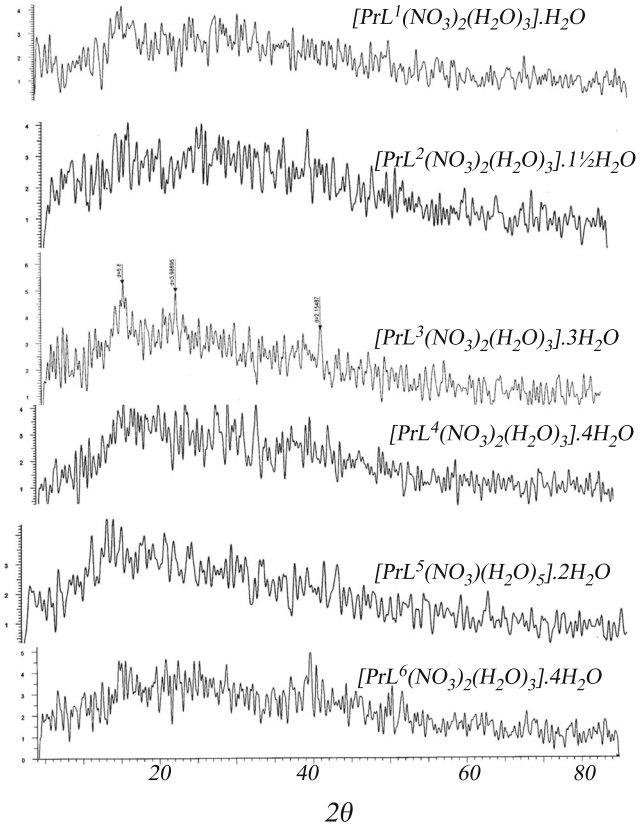

Fig. 1 XRD of the Pr^{3+} complexes of the metformin Schiff-bases

at higher frequency than υ(Pr–N) may be due to large dipole moment change in the vibration of Pr–O band in comparison to that in the Pr–N band [25, 26].

The complex $[PrL^5(NO_3)(H_2O)_5].2H_2O$ has IR data showing υ(NH) and υ(C=N) at 3357, 3224 and 1639, 1572, 1548 cm^{-1}, respectively. These values are different from the rest of the complexes and nearly similar in number and position to the free HL^1 Schiff-base frequencies. This indicates the non-participation of either C=NH or HC=N groups in bonding in the complex. N–C–N is absent in the IR spectrum of this complex. The bands at 1432 cm^{-1} and 1325 cm^{-1} are due to υ(N=O) (υ_5) and $\upsilon_{as}(NO_2)$ (υ_1) of the coordinated nitrate. The $\upsilon_s(NO_2)$ (υ_2) is detected at 1039 cm^{-1}. The magnitude of separation for this complex (Table 2) is indicative of a monodentate nitrate (98 cm^{-1}) [24]. Also, in this complex, υ(C–O) appears as a very strong band at 1288 cm^{-1} while the other complexes showed this band as a medium split one. The nature of metal–ligand bonding is confirmed by the newly formed band at 595 cm^{-1} in the spectra of the complex which is assigned to υ(Pr–O) [27]. Also, Pr^{3+} is a hard acid, so it is expected to prefer bonding through the two oxygen atoms of the hydroxyl groups (hard base) of the Schiff-base after deprotonation forming five membered ring which may be more stable than forming six membered ring through nitrogen atoms [28].

Magnetic and Spectral Properties

The magnetic susceptibility values (Table 4) of the complexes reveal that the Pr^{3+} is paramagnetic with magnetic moment in the 3.7-3.77 B.M. range. These results showed slight deviation from the van Vleck values [29], indicating an insignificant participation of the 4*f* electrons in the bonding.

The tripositive praseodymium ion has the outer configuration $4f^25s^25p^6$ and follows the Russell-Saunders L, S, J coupling scheme, but with a certain amount of configuration interaction. The electronic spectra of Pr(III) can be considered [30] to be derived from the spectra of the gaseous ion by a fairly small perturbation: nephelauxetic and crystal field splitting effects. The spectra of lanthanide ions are composed of closely spaced sharp lines arise from transitions among f^n configuration levels. The 4f electrons of lanthanides are more or less protected from the influence of the lattice by polarization of the $5s^2$ and $5p^6$ closed shells. In the visible region, the absorption spectra of Pr^{3+} in solution involve four bands due to the transitions from the ground state level $^3H_4$ to $^3P_0$, $^3P_1 + {}^1I_6$, $^3P_2$ and $^1D_2$ levels.

The UV–Vis spectra of 10^{-3} and 10^{-5} M of the Pr^{3+} complexes were recorded in DMSO (Table 3 and Figs. S3 and S4 in supplementary file). The $\pi \rightarrow \pi^*$ transitions of the aromatic rings were observed in the 296-251 nm whereas the $n \rightarrow \pi^*$ transitions of the C=N bond are in the 337-318 nm range [31, 32]. As regards the electronic spectra of the obtained complexes, the shifts of the characteristic bands were observed comparable to the HL^1 Schiff-base [11], what confirms complex formation.

The complexes $[PrL^1(NO_3)_2(H_2O)_3].H_2O$, $[PrL^2(NO_3)_2(H_2O)_3].1½H_2O$, $[PrL^4(NO_3)_2(H_2O)_3].4H_2O$, $[PrL^5(NO_3)(H_2O)_5].2H_2O$ and $[PrL^6(NO_3)_2(H_2O)_3].4H_2O$ showed the $^3H_4 \rightarrow {}^3P_2$ transition at 444, 445, 439, 426 and 425 nm, respectively. Also, the transition $^3H_4 \rightarrow {}^3P_1$ of the complexes $[PrL^2(NO_3)_2(H_2O)_3].1½H_2O$ and $[PrL^3(NO_3)_2(H_2O)_3].3H_2O$ was observed at 555 and 463 nm. Finally, the complexes, $[PrL^3(NO_3)_2(H_2O)_3].3H_2O$, $[PrL^5(NO_3)(H_2O)_5].2H_2O$, and $[PrL^6(NO_3)_2(H_2O)_3].4H_2O$ exhibited the $^3H_4 \rightarrow {}^3P_0$ transition in the 482-472 nm range.

Nephelauxetic parameter, β, quantitatively describes the nephelauxetic effect which is absorption band shift towards lower energy on complex formation [33]. It is equal to the ratio of the inter-electron repulsion parameters in the complex and in the free ion [34]:

$$\beta = \frac{\upsilon\ complex}{\upsilon\ free\ ion}$$

Electronic spectra of Pr(III) complexes were recorded and compared with the data for the corresponding aquaions. The covalence parameter, δ, has been calculated using Sinha's expression:

Table 2 IR spectral data of the Pr^{3+} complexes of the metformin Schiff-bases

Compound	υ(H_2O), υ(OH)	υ(NH)	υ(C=N)	υ(N-C-N)	υ(C-O)	NO_3^-			Δυ	υ(Pr-O), υ(Pr-N)
						υ_5	υ_1	υ_2		
$HL^1(C_{11}H_{15}N_5O)$ [11]	3456 br.	3370 s. 3297 s. 3172 s.	1643 s. 1599 s. 1564	1498 m.	1291 m. 1230	—	—	—	—	—
$[PrL^1(NO_3)_2(H_2O)_3].H_2O$	3629 m.s. 3425 m.br.	3204 sh.	1645 s. 1604	1531s.	1186 m.	1445 m	1324 m	1030 m.	121	466 m. 427 m.
$[PrL^2(NO_3)_2(H_2O)_3].1½H_2O$	3572 m.br. 3406 m.br.	3204 br.	1629 s. 1590	1538 m.	1202 s.	1435 m.	1326 m.	1037 m.	109	566 m. 521 m.
$[PrL^3(NO_3)_2(H_2O)_3].3H_2O$	3510 m.br. 3418 m.br.	3204 br.	1604 s. 1590	1540 sh.	1224 m.	1405 m.	1306 m.	1041 m.	99	596 m. 518 m.
$[PrL^4(NO_3)_2(H_2O)_3].4H_2O$	3560 m.br. 3423 s.br.	3200 sh.	1640 s. 1590	1552 sh.	1221 m.	1446 m.	1321 m.	1041 m.	125	563 m. 457 m.
$[PrL^5(NO_3)(H_2O)_5].2H_2O$	3593 m.br. 3438 m.br	3357 br. 3224 sh.	1639 s. 1572 m. 1548	–	1288 vs.	1432 m.	1325 m.	1039 m.	98	595 m. —
$[PrL^6(NO_3)_2(H_2O)_3].4H_2O$	3583 m.br. 3440 m.br.	3218 br.	1623 s. 1587	1550 sh.	1184 m.	1456 m.	1364 m.	1039 m.	92	486 m. 447 m.

s. = strong, vs. = very strong, m. = medium, br. = broad, sh. = shoulder, w. = weak

$$\delta\% = [(1-\beta)/\beta]\text{x}100$$

The bonding parameters ($b^{1/2}$) along with the covalence angular overlap parameter (η) were also calculated using the following formulae [30]:

$$b^{\S} = \S\left[(1-\beta)^{\S}\right]$$

$$\eta = \left[(1-\beta)^{\S}\right]/\beta^{\S}$$

These parameters measure the amount of 4f-ligand mixing, i.e. covalence. The values of these parameters for the reported complexes are given in Table 3. It shows that the metal to ligand bonding is covalent as compared to lanthanide aquo-ions, or that the 4f electrons are more localized [35].

Emission Spectra

The photoluminescence properties of the complexes were investigated in 10^{-3} M DMSO solution at room temperature (Table 4, Figs. S5 and S6 in supplementary file). Because Pr^{3+} can show emission lines originating from three different levels (^3P_o, $^1D_2$ and $^1G_4$) which span the visible and NIR regions, the luminescence spectrum of Pr^{3+} compound is much more complex compared to other Ln^{3+} systems [36]. The complexes exhibited a series of characteristic emission bands for Pr^{3+} ion in the visible region with a 318-332 nm excitation source. The emission in the 590-580 nm range can be assigned to $^1D_2 \rightarrow {}^3H_4$ transitions in all studied complexes. Except the complex $[PrL^2(NO_3)_2(H_2O)_3].1½H_2O$, a series of emission bands centered at approximately 481, 472, 475, 477, and 486 nm were observed corresponding to the $^3P_0 \rightarrow {}^3H_4$ transitions. The two peaks observed at 458 and 457 nm are attributed to the $^3P_1 \rightarrow {}^3H_4$ transition in the complexes $[PrL^3(NO_3)_2(H_2O)_3].3H_2O$ and $[PrL^4(NO_3)_2(H_2O)_3].4H_2O$ spectra. Finally, peaks with a maxima at 442 and 440 nm can be referred to the $^3P_2 \rightarrow {}^3H_4$ transition for the complexes $[PrL^2(NO_3)_2(H_2O)_3].1½H_2O$, $[PrL^5(NO_3)(H_2O)_5].2H_2O$ and $[PrL^6(NO_3)_2(H_2O)_3].4H_2O$.

GC-MS Spectra

GC-MS spectra were recorded that confirm the suggested structure of the Pr(III) complexes. The peaks related to the molar masses of the complexes and its structural fragments are listed in Table 5 (Fig. S7 in supplementary file). The mass spectra of the complexes showed peaks at m/z (calcd./found): 569.1/569.1, 577.1/577.2; 594.1/593.2, 639.1/638.1, 673.1/672.0; and 621.1/622.0 assignable to $[M]^+$; $[M-1]^+$; and $[M+1]^+$ for the complexes $[PrL^1(NO_3)_2(H_2O)_3].H_2O$, $[PrL^5(NO_3)(H_2O)_5].2H_2O$; $[PrL^2(NO_3)_2(H_2O)_3].1½H_2O$, $[PrL^4(NO_3)_2(H_2O)_2].2H_2O$, $[PrL^6(NO_3)_2(H_2O)_3].4H_2O$; and

Table 3 Electronic spectra of the Pr^{3+} complexes of the metformin Schiff-bases

Compound	UV Bands(nm)	Assignment	$\xi*10^3$ $M^{-1}.cm^{-1}$	Covalence parameters
HL^1 ($C_{11}H_{15}N_5O$) [11]	256,295	$\pi \rightarrow \pi^*$	–	–
	343,381	$n \rightarrow \pi^*$		
Pr^{3+} free ion (aq.)	430	$^3H_4 \rightarrow {}^3P_2$ $^3H_4 \rightarrow {}^3P_1$	–	–
	454	$^3H_4 \rightarrow {}^3P_0$		
	468	$^3H_4 \rightarrow {}^1D_2$		
	577			
$[PrL^1(NO_3)_2(H_2O)_3]. H_2O$	260	$\pi \rightarrow \pi^*$	1.94	$\beta = 0.968$
	321	$n \rightarrow \pi^*$	1.09	$b^{1/2} = 0.0887$ $\delta = 3.2558$
	444	$^3H_4 \rightarrow {}^3P_2$	0.0129	$\eta = 0.01614$
$[PrL^2(NO_3)_2(H_2O)_3].1½ H_2O$	251	$\pi \rightarrow \pi^*$	1.38	$\beta_{avg} = 0.982$
	318	$n \rightarrow \pi^*$	0.16	$b^{1/2} = 0.0669$
	445	$^3H_4 \rightarrow {}^3P_2$ $^3H_4 \rightarrow {}^3P_1$	0.013	$\delta = 1.828$
	555		0.003	$\eta = 0.009$
$[PrL^3(NO_3)_2(H_2O)_3].3H_2O$	268	$\pi \rightarrow \pi^*$	0.1361	$\beta = 0.986$
	320	$n \rightarrow \pi^*$	0.0766	$b^{1/2} = 0.0590$
	463	$^3H_4 \rightarrow {}^3P_1$	0.0285	$\delta = 1.415$
	472	$^3H_4 \rightarrow {}^3P_0$	0.0294	$\eta = 0.007$
$[PrL^4(NO_3)_2(H_2O)_3].4H_2O$	296	$\pi \rightarrow \pi^*$	0.403	$\beta = 0.97949$
	337	$n \rightarrow \pi^*$	0.0284	$b^{1/2} = 0.0715$
	439	$^3H_4 \rightarrow {}^3P_2$	0.0096	$\delta = 2.09302$
				$\eta = 0.0104$
$[PrL^5(NO_3)(H_2O)_5].2H_2O$	256	$\pi \rightarrow \pi^*$	0.77	$\beta = 0.99219$
	332	$n \rightarrow \pi^*$	0.28	$b^{1/2} = 0.0441$
	426	$^3H_4 \rightarrow {}^3P_2$	0.016	$\delta = 0.7866$
	480	$^3H_4 \rightarrow {}^3P_0$	0.0087	$\eta = 0.0039$
$[PrL^6(NO_3)_2(H_2O)_3].4H_2O$	276	$\pi \rightarrow \pi^*$	11.16	$\beta_{avg} = 0.991$
	325	$n \rightarrow \pi^*$	22.88	$b^{1/2} = 0.0464$
	425	$^3H_4 \rightarrow {}^3P_2$	0.227	$\delta = 0.87183$
	482	$^3H_4 \rightarrow {}^3P_0$	0.2045	$\eta = 0.0043$

$*10^{-3}$ M in DMSO

$[PrL^3(NO_3)_2(H_2O)_3].3H_2O$, respectively. The patterns of peaks give a clear impression of the successive degradation of the target compound with the series of peaks corresponding to the various fragments with different intensities.

Table 4 Fluorescence spectra and magnetic moment of the Pr^{3+} complexes of the metformin Schiff-bases

Complex	λ_{ex}	λ_{em}	*RLI	Assignment	**μ_{eff} (B.M.)
$[PrL^1(NO_3)_2(H_2O)_3]. H_2O$	321	481	356	$^3P_0 \rightarrow {}^3H_4$	3.75
$[PrL^2(NO_3)_2(H_2O)_3].1½ H_2O$	318	442	13.33	$^3P_2 \rightarrow {}^3H_4$	3.71
		585	2.77	$^1D_2 \rightarrow {}^3H_4$	
$[PrL^3(NO_3)_2(H_2O)_3].3H_2O$	320	458,589	13.33	$^3P_1 \rightarrow {}^3H_4$	3.72
			11.42	$^1D_2 \rightarrow {}^3H_4$	
$[PrL^4(NO_3)_2(H_2O)_3].4H_2O$	320	457	15.37	$^3P_1 \rightarrow {}^3H_4$	3.70
		582	5.46	$^1D_2 \rightarrow {}^3H_4$	
$[PrL^5(NO_3)(H_2O)_5].2H_2O$	332	442	8.5	$^3P_2 \rightarrow {}^3H_4$	3.72
		477	9.6	$^3P_0 \rightarrow {}^3H_4$	
		590	6.43	$^1D_2 \rightarrow {}^3H_4$	
$[PrL^6(NO_3)_2(H_2O)_3].4H_2O$	325	440	8.3	$^3P_2 \rightarrow {}^3H_4$	3.77
		486	11	$^3P_0 \rightarrow {}^3H_4$	
		580	6.2	$^1D_2 \rightarrow {}^3H_4$	

* Relative luminescence intensity

** Room temperature

Table 5 Mass fragmentation pattern of the Pr^{3+} complexes of the metformin Schiff-bases

Complex	m/z calcd. (found) (%)	Abs. Int.	Rel. Int.	Weight loss(%)	Assignments
$[PrL^1(NO_3)_2(H_2O)_3].H_2O$	569.1 (569.1)	60	0.38	—	$[M]^+$
	551.1 (551.1)	305	1.93	H_2O(3.16)	$[Pr(L^1)(NO_3)_2(H_2O)_3]^+$
	533.1 (533.1)	89	0.56	H_2O (3.16)	$[Pr(L^1)(NO_3)_2(H_2O)_2]^+$
	515.1 (515.1)	62	0.39	H_2O (3.16)	$[Pr(L^1)(NO_3)_2(H_2O)]^+$
	497.1 (497.1)	86	0.55	H_2O (3.16)	$[Pr(L^1)(NO_3)_2]^+$
	435.1 (435.1)	105	0.67	NO_3^- (10.88)	$[Pr(L^1)NO_3]^+$
	373.1 (373.1)	116	0.74	NO_3^- (10.88)	$[Pr(L^1)]+$
	328.2 (328.1)	106	0.67	$HN(CH_3)_2$ (7.90)	$[Pr(0.8L^1)]^+$
	266.9 (266.0)	158	1.0	$HN(CH{=}NH)_2$ (12.47)	$[Pr(0.5L^1)]^+$
	140.8(140.1)	471	2.99	$0.5L^1$	$[Pr]^+$
$[PrL^2(NO_3)_2(H_2O)_3].1½H_2O$	594.1 (593.2) 576.1(576.2)	60	0.25	—	$[M–1]^+$
	549.1(549.2)	87	0.36	1½ H_2O (4.54)	$[Pr(L^2)(NO_3)_2(H_2O)_3]^+$
	531.1 (532.2)	406	1.69	H_2O(3.02)	$[Pr(L^2)(NO_3)_2(H_2O)_2]^+$
	513.1 (513.2)	82	0.34	H_2O (3.02)	$[Pr(L^2)(NO_3)_2(H_2O)]^+$
	451.1(454.1)	79	0.33	H_2O (3.02)	$[Pr(L^2)(NO_3)_2]^+$
	389.1(389.1)	346	1.44	NO_3^- (10.43)	$[Pr(L^2)NO_3]^+$
	344.1(344.1)	94	0.39	NO_3^- (10.43)	$[Pr(L^2)]+$
	273.1(273.0)	71	0.3	$HN(CH_3)_2$ (7.57)	$[Pr(0.8L^2)]^+$
	140.8(140.1)	257	1.07	$HN(CH{=}NH)_2$ (11.95)	$[Pr(0.53L^2)]^+$
		713	2.97	$0.53L^2$	$[Pr]^+$
$[PrL^3(NO_3)_2(H_2O)_3].3H_2O$	621.1(622.2)	62	0.4	—	$[M+1]^+$
	603.1(603.2) 585.1(585.2)	66	0.43	H_2O (2.89)	$[Pr(L^3)(NO_3)_2(H_2O)_3]^+ .2H_2O$
	567.1(567.2)	79	0.5	H_2O (2.89)	$[Pr(L^3)(NO_3)_2(H_2O)_3]^+.H_2O$
	549.1(549.2)	63	0.41	H_2O(2.89)	$[Pr(L^3)(NO_3)_2(H_2O)_3]^+$
	451.1 (451.2)	194	1.25	H_2O (2.89)	$[Pr(L^3)(NO_3)_2(H_2O)_2]^+$
	389.1(389.2)	199	1.28	$2H_2O + NO_3^-$(15.77)	$[Pr(L^3)NO_3]^+$
	344.1(344.1)	52	0.34	NO_3^- (9.97)	$[Pr(L^3)]+$
	273.1(273.1)	74	0.48	$HN(CH_3)_2$ (7.24)	$[Pr(0.8L^3)]^+$
	140.8(140.1)	129	0.83	$HN(CH{=}NH)_2$ (11.43)	$[Pr(0.53L^3)]^+$
		564	3.6	$0.53L^3$	$[Pr]^+$
$[PrL^4(NO_3)_2(H_2O)_3].4H_2O$	639.1 (638.1)	71	0.56	—	$[M–1]^+$
	621.1(621.1)	70	0.55	H_2O (2.81)	$[Pr(L^4)(NO_3)_2(H_2O)_3]^+.3H_2O$
	603.1(603.1)	66	0.52	H_2O (2.81)	$[Pr(L^4)(NO_3)_2(H_2O)_3]^+.2H_2O$
	585.1(585.1)	54	0.42	H_2O (2.81)	$[Pr(L^4)(NO_3)_2(H_2O)_3]^+.H_2O$
	567.1(567.1)	95	0.75	H_2O (2.81)	$[Pr(L^4)(NO_3)_2(H_2O)_3]^+$
	513.1(513.1)	58	0.46	$3H_2O$(8.44)	$[Pr(L^4)(NO_3)_2]^+$
	451.1 (451.1)	100	0.78	NO_3^- (18.14)	$[Pr(L^4)(NO_3)]^+$
	389.1(389.1)	66	0.52	NO_3^- (9.69)	$[Pr(L^4)]^+$
	344.1(344.0)	84	0.66	$HN(CH_3)_2$(7.04)	$[Pr(0.81L^4)]^+$
	273.1(273.1)	121	0.95	$HN(CH{=}NH)_2$(11.1)	$[Pr(0.53L^4)]^+$
	140.8(140.1)	535	4.2	$0.53L^4$	$[Pr]^+$
$[PrL^5(NO_3)(H_2O)_5].2H_2O$	577.1(577.2)	238	0.7	—	$[M]^+$
	559.1(559.2)	71	0.21	H_2O (3.1)	$[Pr(L^5)\ NO_3(H_2O)_5]^+.2H_2O$
	541.1(541.1)	66	0.19	H_2O (3.1)	$[Pr(L^5)\ NO_3(H_2O)_5]^+.\ H_2O$
	523.1(523.1)	487	1.43	H_2O (3.1)	$[Pr(L^5)\ NO_3(H_2O)_4]^+$
	505.1(505.1)	79	0.23	H_2O (3.1)	$[Pr(L^5)\ NO_3(H_2O)_3]^+$
	451.1(451.1)	244	0.72	$3H_2O$ (9.3)	$[Pr(L^5)\ NO_3]^+$
	389.1(389.1)	79	0.23	NO_3^- (10.7)	$[Pr(L^5)]^+$
	344.1(344.0)	70	0.21	$HN(CH_3)_2$ (7.7)	$[Pr(0.8L^5)]^+$
	273.1(273.8)	132	0.39	$HN(CH{=}NH)_2$ (12.3)	$[Pr(0.53L^5)]^+$
	140.2(140.0)	74	2.19	$0.53L^5$	$[Pr]^+$
$[PrL^6(NO_3)_2(H_2O)_3].4H_2O$	673.1 (672.0)	60	0.25	—	$[M–1]^+$
	655.1 (655.2)	79	0.33	H_2O (2.67)	$[Pr(L^6)(NO_3)_2(H_2O)_3]^+.3H_2O$
	637.1(637.2)	60	0.66	H_2O (2.67)	$[Pr(L^6)(NO_3)_2(H_2O)_3]^+.2H_2O$
	619.1(619.2)	54	0.22	H_2O (2.67)	$[Pr(L^6)(NO_3)_2(H_2O)_3]^+.H_2O$
	601.1(601.2)	84	0.35	H_2O (2.67)	$[Pr(L^6)(NO_3)_2(H_2O)_3]^+$
	583.1(583.2)	84	0.53	$3H_2O$ (8.02)	$[Pr(L^6)(NO_3)_2]^+$
	547.1(547.2)	158	0.66	NO_3^- (9.20)	$[Pr(L^6)NO_3]^+$
	485.1(485.1)	65	0.27	NO_3^- (9.20)	$[Pr(L^6)]^+$
	423.2(423.0)	585	2.43	$HN(CH_3)_2$ (6.68)	$[Pr(0.84L^6)]^+$
	378.2(378.1)	87	0.36	$HN(CH{=}NH)_2$(10.54)	$[Pr(0.58L^6)]^+$
	307.2(307.1)	153	0.64	$0.58L^6$	$[Pr]^+$

Table 6 TGA and DTG data of the Pr^{3+} complexes of the metformin Schiff-bases

Compound	Temp. range C	DTG C	Mass loss%		Process	Product	Residue% and type
			Found	Calcd.			Found(Calcd.).
$HL^1(C_{11}H_{15}N_5O)$ [11]	160-293	314	19.17	19.29	Partial decomposition	$HN(CH_3)_2$	20.1(19.29)
	294-422	449	30.14	30.43	Ligand decomposition	HN(CH=NH)2	Carbonaceous material
	423-600	556	30.25	30.32	Final decomposition	0.13 L	
$[PrL^1(NO_3)_2(H_2O)_3].H_2O$	28-171	112	3.37	3.16	Dehydration	H_2O	49.07
	250-350	314	10.97	11.06	Coordinated nitrate	HNO_3	(28.97 Pr_2O_3
	360-480	449	28.57	28.46	Partial decomposition	$3H_2O + HNO_3 + HN(CH_3)_2$	+ carbonaceous material)
	520-585	556	7.01	7.73	Final decomposition	CO_2	
$[PrL^2(NO_3)_2(H_2O)_3].1½H_2O$	28-177	68	4.25	4.54	Dehydration	$1½H_2O$	38.12
	179-402	298	27.39	27.25	Partial decomposition	$2H_2O + 2HNO_3$	(27.75 Pr_2O_3
	415-605	461	22.96	22.55	Partial decomposition	$H_2O + HN(CH_3)_2$	+ carbonaceous material)
		521	7.28	7.4	Final decomposition	$HN(CH=NH)_2$ CO_2	
$[PrL^3(NO_3)_2(H_2O)_3].3H_2O$	19-184	61	8.5	8.69	Dehydration	$3H_2O$	37.1
	163-371	290	20.28	20.27	Coordinated nitrate	$2HNO_3$	(26.54 Pr_2O_3
	373-686	464, 534	33.6	34.45	Partial decomposition	$3H_2O + HN(CH_3)_2$ $HN(CH=NH)_2 + CO_2$	+ carbonaceous material)
$[PrL^4(NO_3)_2(H_2O)_3].4H_2O$	18-137	61	13.3	11.26	Dehydration	$4H_2O$	40.0
	163-351	267	15.7	15.48	Coordination sphere	$2H_2O + HNO_3$	(25.8 Pr_2O_3
	390-661	514	30.05	30.81	Partial decomposition	$H_2O + HNO_3 + HN(CH_3)_2$ $+ HN(CH=NH)_2$	+ carbonaceous material)
$[PrL^5(NO_3)(H_2O)_5].2H_2O$	20-197	66	9.58	9.37	Dehydration	$3H_2O$	39.12
	198-350	285	17.88	17.01	Coordination sphere	$2H_2O + HNO_3$	(28.62 Pr_2O_3
	375-435	406	26.12	26.38	Partial decomposition	$2H_2O + HN(CH_3)_2$	+ carbonaceous material
	630-665	640	8.2	7.63	Final decomposition	$+ HN(CH=NH)_2$ CO_2	
$[PrL^6(NO_3)_2(H_2O)_3].4H_2O$	28-165	89	10.38	10.69	Dehydration	$4H_2O$	42.0
	242-350	298	12.12	12.02	Coordination sphere	$H_2O + HNO_3$	(24.49 Pr_2O_3
	395-640	521	32.13	31.93	Partial decomposition	$2H_2O + HNO_3 + HN(CH_3)_2$	+ carbonaceous material)
	690-875	750	3.12	3.26	Solid state reaction	$+ HN(CH=NH)_2$ $½CO_2$	

Thermal Analysis

Thermal analysis of the Pr(III) complexes was performed in order to study the nature of water in the investigated compounds, their thermal stability, as well as decomposition modes under controlled heating rate. The measurements were taken in nitrogen atmosphere within 25–750 and 25-1000 °C range at a heating rate of 10 °C min^{-1}. The thermal decomposition data are collected in Tables 6 and 7, and Fig. 2 presents, as an example, the thermoanalytical curves.

Thermal decomposition of the complexes in N_2 atmosphere begins in the 28-171, 28-177, 19-184, 18-137, 20-197 and 28-165 °C range with DTG_{max} at 112, 68, 61, 61, 66 and 89 °C, respectively. It is associated with the release of all hydrated water molecules. Calculated mass loss for the dehydration processes are 3.16, 4.54, 8.69, 11.26, 9.37, and 10.69%, when these were determined from the thermogravimetric curves are 3.37, 4.25, 8.5, 13.3, 9.58, and 10.38%, respectively. This step is confirmed with endothermic DTA_{max} at 113, 71, 61, 67, 73, and 89 °C, respectively, where values of the enthalpy changes are in the range 0.868-2.304 kJ/mol.

In the second decomposition step, evaporation of the coligands of the coordination sphere takes place. The complexes $[PrL^1(NO_3)_2(H_2O)_3].H_2O$;$[PrL^3(NO_3)_2(H_2O)_3].3H_2O$; $PrL^6(NO_3)_2(H_2O)_3].4H_2O$; $[PrL^4(NO_3)_2(H_2O)_3].4H_2O$, $[PrL^5(NO_3)(H_2O)_5].2H_2O$; and $[PrL^2(NO_3)_2(H_2O)_3].1½H_2O$ lose the following species: HNO_3; $2HNO_3$; $H_2O + HNO_3$; $2H_2O + HNO_3$;$2H_2O + HNO_3$; and $2H_2O + 2HNO_3$, respectively. It happens in the temperature range of 250-350; 163-371; 242-350; 163-351; 198-350; and 179-402 °C with DTG_{max} at 314; 290; 298; 267; 285; and 298 °C, respectively. Observed mass reduction in this step is (found/calcd.%): 10.97/11.06%; 20.28/20.27%, 12.12/12.02%; 15.7/15.48%, 17.88/17.01%; and 27.39/27.25% accompanied with exothermic DTA_{max} at 310; 292; 297; 277; 291; and 319 °C, respectively.

Vaporization of the remaining co-ligands as well as oxidative degradation of the Schiff-bases takes place in the third decomposition stage. This step is clearly presented on the DTG curves in the 360-480; 373-686; 395-640; 390-661, 375-435; and 415-605 °C period with DTG_{max} at 449; 464; 521; 514, 406; and 461 °C, respectively, for the above series of complexes. Observed mass lowering are 28.57; 33.6;

Table 7 DTA data of the Pr^{3+} complexes of the metformin Schiff-bases

Compound	Temp. rang. °C	DTA peak	ΔH J/g	Process
$HL^1(C_{11}H_{15}N_5O)$ [11]	160-213 253-351 507-560	195 endo. 290 exo. 531 exo.	89 −190 - 210	Melting Partial decomposition Final decomposition
$[PrL^1(NO_3)_2(H_2O)_3].H_2O$	28-150 260-370 370-550	113 endo 310 exo. 456 exo.	+128 −187 – 5350	Dehydration Coordination sphere Partial decomposition
$[PrL^2(NO_3)_2(H_2O)_3].1½H_2O$	30-160 200-350 390-650	71 endo. 319 exo. 464, 510 exo.	+101 −168 –3320	Dehydration Partial decomposition Final decomposition
$[PrL^3(NO_3)_2(H_2O)_3].3H_2O$	26-180 200-350 380-650	61 endo. 292 exo. 490 exo.	+181 −914 –2120	Dehydration Coordination sphere Partial decomposition
$[PrL^4(NO_3)_2(H_2O)_3].4H_2O$	28-160 170-350 380-650	67 endo. 277 exo. 495 exo.	+360 −704 −1910	Dehydration Coordination sphere Partial decomposition
$[PrL^5(NO_3)(H_2O)_5].2H_2O$	28-150 200-350 360-500	73 endo. 291 exo. 410 exo.	+ 248 −1320 −1920	Dehydration Coordination sphere Partial decomposition
$[PrL^6(NO_3)_2(H_2O)_3].4H_2O$	25-150 235-350 390-590	89 endo. 297 exo. 510, 596 exo.	+193 – 487 −1670	Dedydration Coordination sphere Partial decoposition

32.13; 30.05, 26.12; and 22.96% against calculated mass of 28.46; 34.45; 31.93; 30.81, 26.38; and 22.55%, respectively. It connects with peaks on the exothermic DTA curve at 456; 490; 510; 495, 410; and 464 °C, respectively. The complexes $[PrL^1(NO_3)_2(H_2O)_3].H_2O$, $[PrL^2(NO_3)_2(H_2O)_3].1½H_2O$, $[PrL^5(NO_3)(H_2O)_5].2H_2O$ and $[PrL^6(NO_3)_2(H_2O)_3].4H_2O$ show the evolution of CO_2 in the final degradation process which are recorded at 556, 521, 640 and 750 °C, respectively. Exothermic DTA peaks -showing this step- are observed at 510 and 596 °C only for the complexes $[PrL^2(NO_3)_2(H_2O)_3].1½H_2O$ and $[PrL^6(NO_3)_2(H_2O)_3].4H_2O$.

The solid residues obtained during thermal decomposition are higher than expected for metal oxides. It suggests that the

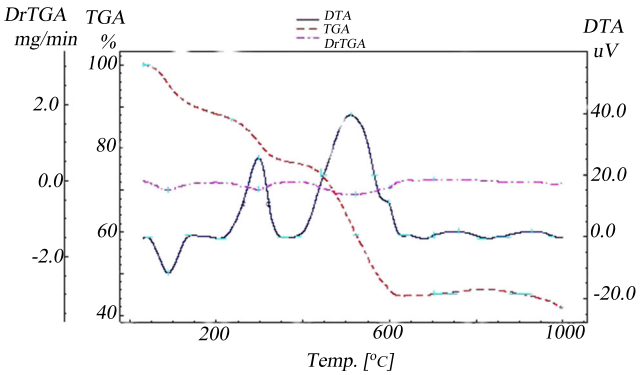

Fig. 2 TGA, DTG and DTA of the complex $[PrL^2(NO_3)_2(H_2O)_3].1½H_2O$

decomposition of the mentioned complexes in nitrogen atmosphere leads probably to appropriate metal oxide and 10.37-20.1% carbon as a final product, what is characteristic for investigations carried out in N_2 atmosphere [37]. This is confirmed using previous TGA analysis on HL^1 Schiff-base which showed that about 20% of carbonaceous material was obtained at 750 °C [11].

Mechanism of Thermal Decomposition

The IR spectrum of the complex $[PrL^4(NO_3)_2(H_2O)_3].4H_2O$ heated at 110, 370 and 600 °C is shown in Fig. 3, in an attempt to elucidate the mechanism of thermal decomposition. It shows that the IR spectrum changes shape, intensity and position of some characteristic bands. Heating the complex at 110 °C, its IR spectrum shows the disappearance of the broad bands at 3560 and 3423 cm^{-1} indicating dehydration [26]. Also, a medium broad band shown at 3377 cm^{-1} may be due to coordinated water. The υ(NH) band is shifted to 3206 cm^{-1} ; $υ(CH)_3$ is observed at 2914 cm^{-1} besides υ(C=N) appears as a sharp split band with maximum at 1630, 1586 and 1543 cm^{-1}. Heating the complex at 370 °C, the bands due the nitrate ion at 1446, 1321, and 1041 cm^{-1} were disappeared which means evolution of one nitrate ion as HNO_3. The υ(C=N) is shifted to 1619 cm^{-1} and new band at 1400 cm^{-1} may be due to the presence of the second nitrate ion. Heated complex at 600 °C shows IR spectrum with

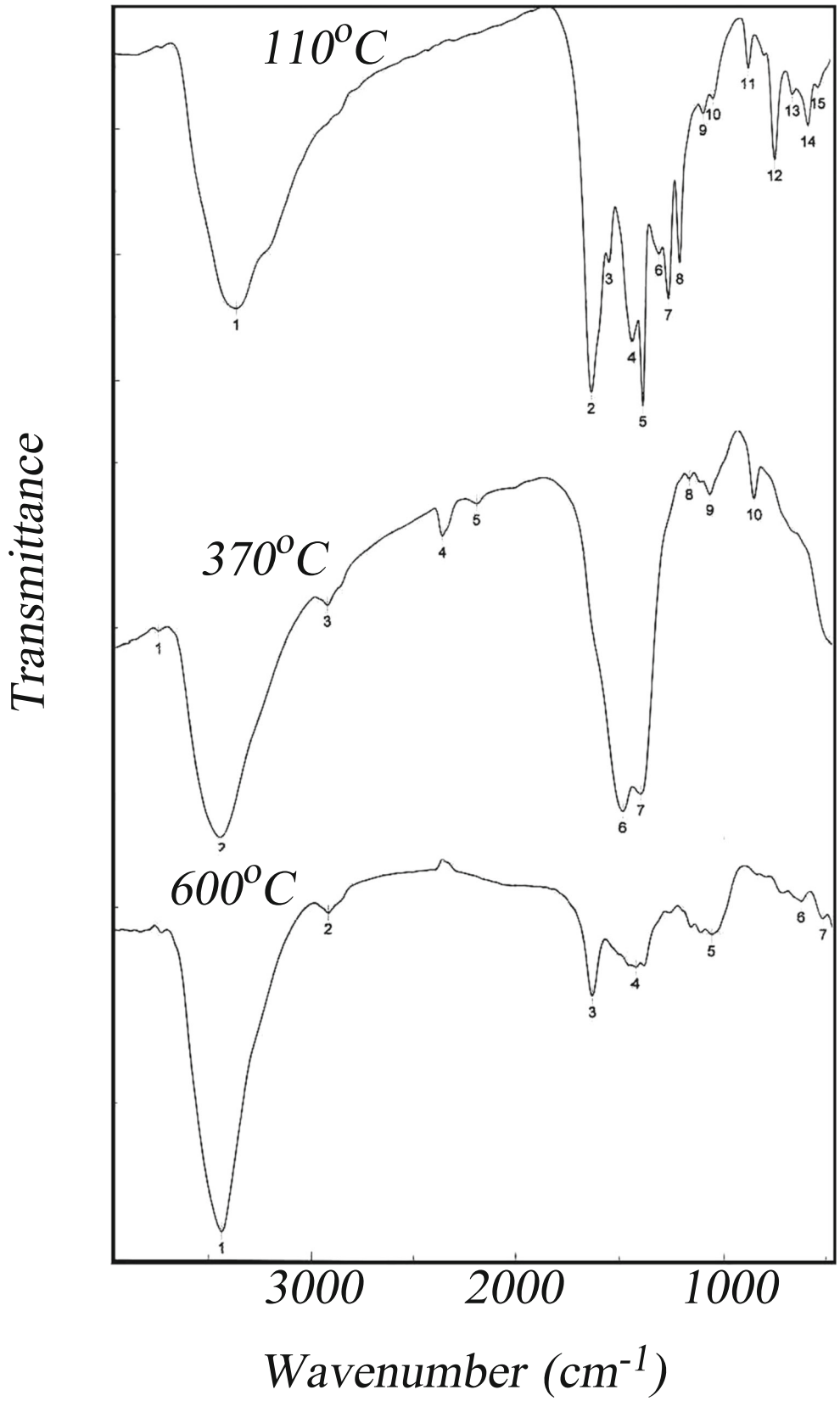

Fig. 3 IR spectrum of the complex $[PrL^4(NO_3)_2(H_2O)_3].4H_2O$ at different temperatures

distinct band of $\upsilon(CH_3)$ at 2924 cm^{-1} was not observed indicating cleavage of the ligand at the metformin part of the Schiff-base and evolution of $NH(CH_3)_2$ species. Also, the strong band at 1619 cm^{-1} is absent referring to the

Table 8 Kinetic parameters for the second decomposition step for the Pr^{3+} complexes of the metformin Schiff-bases

Compound	T_{max}	ΔE_a	Z	n	r	ΔH	ΔS	ΔG
$[PrL^1(NO_3)_2(H_2O)_3].H_2O$	314	37.4	$2.0*10^4$	0.5	0.983	32.6	−163.9	131.1
$[PrL^2(NO_3)_2(H_2O)_3].1½H_2O$	298	41.0	$2.2*10^{*4}$	0.33	0.989	36.3	−167.0	131.6
$[PrL^3(NO_3)_2(H_2O)_3].3H_2O$	290	85.6	$4.1*10^4$	2	0.996	80.9	−161.8	172.0
$[PrL^4(NO_3)_2(H_2O)_3].4H_2O$	267	59.6	$3.1*10^4$	2	0.999	55.1	−163.8	143.5
$[PrL^5(NO_3)(H_2O)_5].2H_2O$	285	109.2	$4.7*10^4$	2	0.980	104.5	−160.6	194.2
$[PrL^6(NO_3)_2(H_2O)_3].4H_2O$	298	64.4	$3.3*10^4$	2	0.992	59.6	−167.9	153.1

ΔE_a, ΔH, ΔG in kJ/mol

ΔS in JK^{-1} mol^{-1}

Z in S^{-1}

decomposition of the azomethine υ(C=N) of the Schiff-base. Appearance of new bands at 3435, 2922 and 1633 cm^{-1} in the IR spectrum of heated sample at 600 °C may be assigned to υ(OH), υ(CH_2) and δ(OH) which refer to the formation of a mixture of aqua-hydroxo species and some carbonaceous material [38]. Characteristic IR bands for the presence of Pr_2O_3 is shown as split medium band at 1061 and 515 cm^{-1} which is representing υ(Pr − O) [39]. Proposed mechanism of thermal decomposition of the complex $[PrL^4(NO_3)_2(H_2O)_3].4H_2O$ is shown as follows:

Kinetic and Thermodynamic Parameters

The kinetic and thermodynamic parameters including: n (order of reaction), E_a (energy of activation), z (pre-exponential factor), ΔH activation enthalpy, ΔS (entropy of activation) and ΔG (free energy change) together with correlation coefficient r for non-isothermal decomposition of metal complexes have been determined by Coats-Redfern integral method [40]. The data are given in Table 8. The negative values of entropy of activation indicate that the activated complexes are more ordered than the reactants and that the reactions are slow [41]. The more ordered nature may be due to the polarization of bonds in activated state which might happen through charge transfer electronic transition.

The heat of activation ΔE_a, the activation enthalpies ΔH and the free energy of activation ΔG, for the complex $[PrL^6(NO_3)_2(H_2O)_3].4H_2O$ is higher than that for the complex $[PrL^1(NO_3)_2(H_2O)_3].H_2O$ (64.4 > 37.4; 59.6 > 37.4; and 153.1 > 131.1) which reflects the rigid structure of the Schiff-base in the first complex due to the presence of the naphthyl ring. Values of activation energy, activation enthalpy and activation free energy of the second decomposition process of the isostructureal complexes $[PrL^2(NO_3)_2(H_2O)_3].1½H_2O$, $[PrL^3(NO_3)_2(H_2O)_3].3H_2O$ and $[PrL^4(NO_3)_2(H_2O)_3].4H_2O$ have the following order: ΔEa: 41 < 85.6 > 59.6; ΔH: 36.3 < 80.9 > 55.1 and ΔG: 131.6 < 172.0 > 143.5. The high values of ΔE_a, ΔH and ΔG for the complex $[PrL^3(NO_3)_2(H_2O)_3].3H_2O$ may correlate to its capability of strongly hydrogen bonding through m-OH of the H_2L^3 Schiff-base.

Structure of the Complexes

The complex structure has one Pr^{3+} at the center of hexagon surrounded by N, N, O of the Schiff-base besides O, O, O of three H_2O groups and O, O of two NO_3^- groups at the apexes in hexagonal bipyramid stereochemistry (Structure 2). Other eight coordinated geometries include cube, square prism, dodecahedron, bicapped octahedron, bicapped trigonal prism, end-bicapped trigonal prism, and end-bicapped trigonal antiprism [42].

Pr-Metformin Complexes as Indicators for Neutral Sugars

Sensing glucose is very important in the food and pharmaceutical industries. In addition, glucose monitoring is especially critical

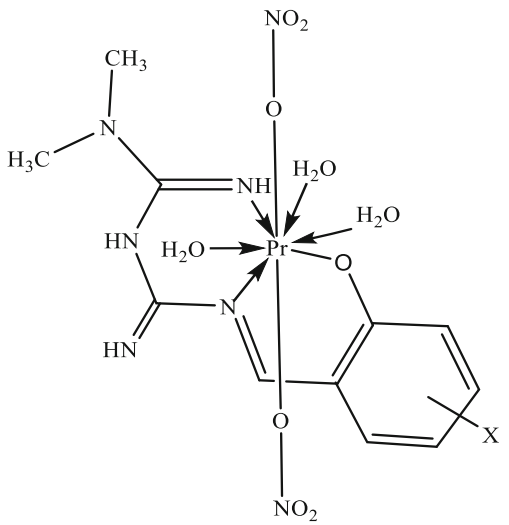

Structure 2 Hexagonal bibyramide stereochemistry of the Pr^{3+} complexes of the metformin Schiff-bases

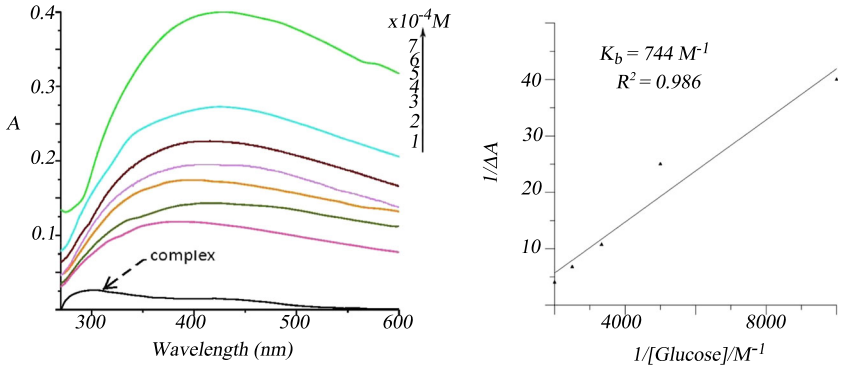

Fig. 4 UV-Vis spectra of the complex $[NdL^2(NO_3)_2(H_2O)_3].3H_2O$ (10^{-4} M) in presence of increasing amounts of glucose (1×10^{-4} M–7×10^{-4} M) using phosphate buffer (pH 7.4)

for diabetes management. Diabetes is characterized by long-term hyperglycemia, and the monitoring of patients' glucose levels is required for the management of the disease. The electrochemical method for sensing glucose is widely used among diabetes patients in the form of a blood glucose meter [43].

Fluorescence of the lanthanide complexes is much more sensitive even to weak interaction with saccharides and has been suggested to detect and identify neutral sugars including cancer biomarkers [44]. The interaction and specificity can be conveniently tuned by varying the metal and/or ligands [45–47]. For many metal complexes, the affinity to sugars and consequent stability constants are comparable to the older and still more common carbohydrate sensors based on the boronic acid [48].

Since the complexes under study contain coordinated water molecules, they are expected to be readily replaced by the deprotonated hydroxyl groups of the incoming sugar. We hypothesize that our Pr-metformin Schiff-base complexes may be useful for detecting sugars in neutral aqueous media which was followed using UV-Vis and fluorescence spectra in addition to viscosity measurements.

Absorption Characteristics of Glucose-Pr Complexes Interaction

The absorption spectra of the interaction of glucose with the Pr(III) complexes have been recorded in aqueous solution of phosphate buffer of pH 7.4 at a constant complex concentration (10^{-4} M). It is apparent that increasing the glucose concentration from 1×10^{-4} M to 8×10^{-4} M leads to moving of the complex band to the 275-428 nm recording red shift of 6 and 5 nm for the complexes $[PrL^5(NO_3)(H_2O)_5].2H_2O$ and $[PrL^6(NO_3)_2(H_2O)_3].4H_2O$ and a blue shift of 5 and 14 nm for the complexes $[PrL^1(NO_3)_2(H_2O)_3].H_2O$ and $[PrL^3(NO_3)_2(H_2O)_3].3H_2O$ associated with hyperchromism (Fig. 4 and Table 9).

The binding constant K_b was calculated based on the double-reciprocal relations assuming the formation of a 1:1 host-guest complex [49].

$$1/\Delta A = 1/\Delta\varepsilon[\text{complex}]_o + 1/K[\text{glucose}]_o\Delta\varepsilon[\text{complex}]_o$$

Where ΔA is the difference between the absorbance of complex in the presence and absence of glucose, Δε is the difference between the molar absorption coefficients of glucose and the complex. $[\text{glucose}]_o$ and $[\text{complex}]_o$ are the initial concentration of glucose and the complex. The intrinsic binding constants K_b of the complexes are in the 567-896 M^{-1} range with a correlation coefficient in the 0.978-0.998 range (Table 9).

Fluorescence Spectra of Glucose-Pr Complexes Mixtures

Since most glucose sensors are fluorescence for the detection, we measured the luminescence spectra for solutions of the free complexes and their mixtures with variable concentrations of glucose. On excitation with λ = 293 nm, glucose exhibit a

Table 9 Binding constants (K_b M^{-1}) of the interaction between the Pr^{3+} complexes of the metformin Schiff base and glucose

Compound	UV				Fluorescence			
	$\lambda_{mix.}$	Δλ	K_b M^{-1}	R-squared	$\lambda_{mix.}$	Δλ	K_b M^{-1}	R-squared
$[PrL^1(NO_3)_2(H_2O)_3].H_2O$	320	−5	632	0.978	482	−4	642	0.989
$[PrL^2(NO_3)_2(H_2O)_3].1½\ H_2O$	425	–	796	0.985	430	2	761	0. 988
$[PrL^3(NO_3)_2(H_2O)_3].3H_2O$	428	−14	744	0.986	338	−4	741	0.976
$[PrL^4(NO_3)_2(H_2O)_3].4H_2O$	403	–	793	0.994	439	_	767	0.981
$[PrL^5(NO_3)(H_2O)_5].2H_2O$	370	6	567	0.998	441	−15	555	0.988
$[PrL^6(NO_3)_2(H_2O)_3].4H_2O$	275	5	896	0.979	434	_	906	0.979

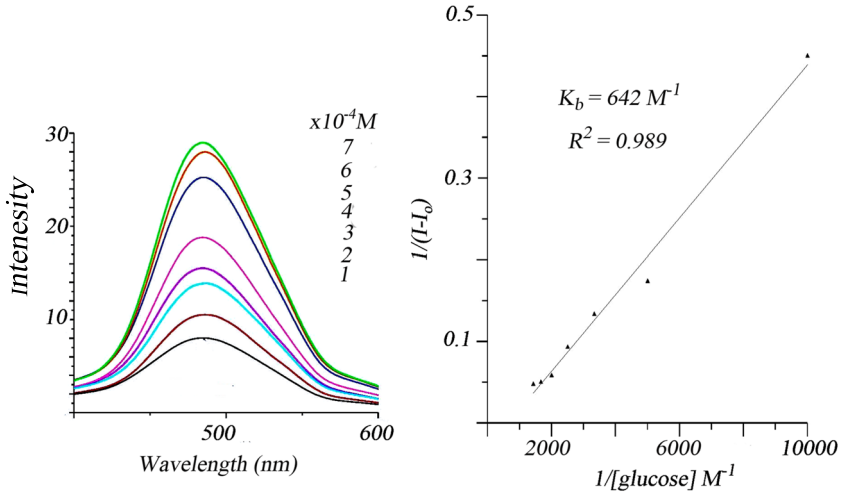

Fig. 5 Fluorescence spectra of the complex $[PrL^1(NO_3)_2(H_2O)_3].H_2O$ (10^{-4} M, λ_{ex} = 293 nm) in presence of increasing amounts of glucose (1×10^{-4} M–7×10^{-4} M) using phosphate buffer (pH 7.4)

weak fluorescence emission at λ = 358 nm. Accordingly, addition of glucose (1×10^{-4} M-7×10^{-4} M) causes a remarkable increase of the complexes fluorescence emission from 338 to 482 nm accompanied by hyperchromism and a red shift of 2 nm for the complex $[PrL^2(NO_3)_2(H_2O)_3].1^1/_2H_2O$ and a blue shift of 4, 4 and 15 nm for the complexes $[PrL^1(NO_3)_2(H_2O)_3].H_2O$, $[PrL^3(NO_3)_2(H_2O)_3].3H_2O$ and $[PrL^5(NO_3)(H_2O)_5].2H_2O$ (Table 9 and Fig. 5).

The binding constants of the complexes (10^{-4} M) with variable concentrations of glucose can be obtained from Benesi-Hildebrand plot, which is double reciprocal type plot of $1/(I\text{-}I_o)$ vs. 1/[glucose], where I_o and I are the fluorescence intensities in the absence (free complex) and presence of the glucose, $[glucose]_o$ is the analytical concentration of glucose, and I_1 is the limiting intensity of fluorescence [49]. The binding constant (K_b) is the association constant for 1:1 complex which can be calculated from the fluorescence data based on the following equation:

$$1/(I\text{–}I_o) = 1/(I_1\text{–}I_o)K[glucose]_o + 1/I_1\text{–}I_o$$

where I_1 is the limiting intensity of fluorescence. Thus the K_b value was obtained from the slope and the intercept of the plot. The values of binding constant of the Pr^{3+} complexes are in the range of 555-906 M^{-1} with a correlation coefficient in the 0.976-0.989 range. The obtained K_b value is in reasonable agreement with that obtained from UV-Vis absorption data.

Water-soluble salophene–La^{3+} complex forms 1:1 stoichiometry with glucose, maltose and maltotriose exhibiting binding constants of 500, 1.666 and 2.500 M^{-1}, respectively [47]. The $K_{eq\text{-}tet}$ for the glucose-PBA (phenyl boronic acid) complex calculated using pH-depression method was 110 M^{-1}. With the ARS method, the $K_{eq\text{-}tet}$ for the glucose was 77 M^{-1} at pH 7.5 [50]. A novel conjugate of phenylboronic acid and an La(DTPA) derivative, in which the central acetate pendant arm was replaced by the methylamide of L-lysine, interacts with glucose at 25 °C having thermodynamic stability constant of 712 M^{-1} using ^{11}B NMR technique [51]. The calculated K_b values show the good binding ability of the Pr(III) complexes to glucose at pH 7.4 which can be used in diabetes management. This may be obtained through substitution of the coordinated water by glucose molecule. The highest K_b value obtained for the complex $[PrL^6(NO_3)_2(H_2O)_3].4H_2O$ (896 and 906 M^{-1}) may be due to the presence of naphthyl ring in the Shiff-base ligand of the complex. The obtained relatively low K_b value for the complex $[PrL^1(NO_3)_2(H_2O)_3].H_2O$ (632 and 642 M^{-1}) may be due to the absence of a second o-OH group in the Schiff-base ligand which can be substituted by the glucose molecule. The K_b values for the complexes $[PrL^2(NO_3)_2(H_2O)_3].1\frac{1}{2}H_2O$, $[PrL^3(NO_3)_2(H_2O)_3].3H_2O$ and $[PrL^4(NO_3)_2(H_2O)_3].4H_2O$ ($796 > 744 < 793$ M^{-1} and $761 > 741 < 767$ M^{-1}) may correlate with the position of the second –OH group in the phenyl ring of the Schiff-base (o-, m- and p-substituted). The complex $[PrL^5(NO_3)(H_2O)_5].2H_2O$ have the lowest K_b value (567 and 555 M^{-1}). In this complex Pr^{3+} is strongly coordinated to two O atoms of the hydroxyl groups of the Schiff-bases which reflected in a weak bonding with the interacting glucose molecule.

Viscosity Measurements

Relative viscosities for glucose in the presence and absence of the complexes were calculated from the relation:

$$\eta = (t\text{–}t_o)/t_o$$

where t is the observed flow time of glucose containing solution and t_o is the flow time of phosphate buffer alone. Data are presented as $(\eta/\eta_o)^{1/3}$ versus binding ratio r (r = [complex]/[glucose]), where η is the viscosity of glucose in the presence of complex and η_o is the viscosity of glucose alone. Titration were performed by the addition of $1\text{-}8 \times 10^{-5}$ M and $1\text{-}8 \times 10^{-4}$ M of the glucose to a constant solution of the complexes ($1\text{-}8X10^{-5}$ M and $1\text{-}8 \times 10^{-4}$ M).

Viscosity measurements of the complexes were carried out, and the effect of the glucose on the viscosity of the complexes is shown in Fig. 6 (representative example). As shown in Fig. 6, the increase in the concentration of the glucose caused an increase in the viscosity of complexes. Thus, it can be concluded that the Pr-metformin complexes, certainly, is a glucose binder.

Conclusion

In order to improve the biological activity of MF (oral hypoglycemic agent) and referring to the biological relevance of lanthanide elements, a series of praseodymium complexes with Schiff-bases of MF with salicylaldehyde (HL^1); 2,3-dihydroxybenzaldehyde (H_2L^2); 2,4-dihydroxybenzaldehyde (H_2L^3); 2,5-dihydroxybenzaldehyde (H_2L^4); 3,4-dihydroxybenzaldehyde (H_2L^5); and 2-hydroxynaphthaldehyde (HL^6) were synthesized by template reaction. The resulting complexes were characterized using elemental analysis, conductivity measurements, magnetic moment, spectral analysis (UV–Vis, fluorescence, IR, GC-MS, XRD), and TG, DTG and DTA. The complexes exhibit a series of characteristic emission bands for Pr^{3+} ion in the 481-472 and 590-580 nm range with a 318-332 nm excitation source. Schiff-bases are tridentate where Pr^{3+} is bonded through –OH, azomethin C=N and C=NH (metformin), three coordinated water molecules and two nitrate ions forming eight coordinated complex. On the other hand, H_2L^5 ligand is coordinated to Pr^{3+} using –OH groups -ortho to each other- on the phenyl ring of the ligand. Magnetic and spectral data show hexagonal bipyramide stereochemistry for the complexes. Thermal properties confirm the structure of the complexes with proposed thermal decomposition mechanism. Kinetic and thermodynamic parameters were calculated using Coats-Redfern equation. Biological activity of the complexes was evaluated by studying the interaction of these complexes with glucose in phosphate buffer solution using UV-Vis and fluorescence spectra as well as viscosity measurements. The K_b values indicate the good ability of the Pr^{3+} complexes to bind glucose in phosphate buffer medium at pH 7.4.

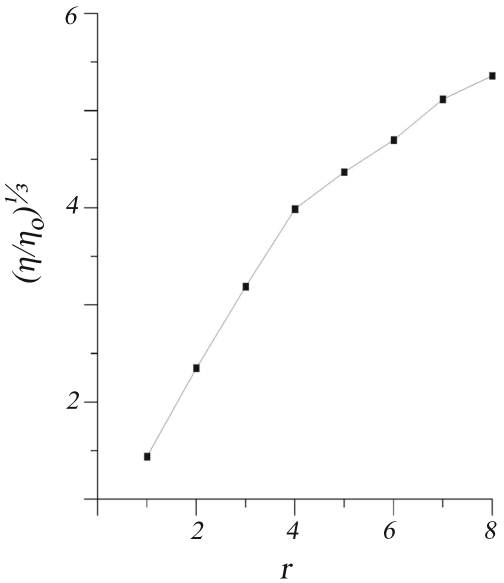

Fig. 6 Effect of increasing amounts of glucose (1×10^{-5} M-8×10^{-5} M) on the viscosity of the complex $[PrL^2(NO_3)_2(H_2O)_3].1½H_2O$ (10^{-5} M) using phosphate buffer (pH = 7.4)

References

1. Stepensky D, Friedman M, Srour W, Raz I, Hoffman A (2001) Preclinical evaluation of pharmacokinetic–pharmacodynamic rationale for oral CR metformin formulation. J Control Release 71:107–115
2. Babykutty PV, Parbhakaran CP, Anantaraman R, Nair CGR (1974) Electronic and infrared spectra of biguanide complexes of the 3d-transition metals. J Inorg Nucl Chem 36:3685–3688
3. Subasinghe S, Greenbaum AL, McLean P (1985) The insulin-mimetic action of Mn^{2+}: involvement of cyclic nucleotides and insulin in the regulation of hepatic hexokinase and glucokinase. Biochem Med 34:83–92
4. Zhu M, Lu L, Yang P, Jin X (2002) Bis(1,1-dimethylbiguanido)copper(II) octahydrate. Acta Crystallogr E58: m217–m219
5. Patrinoiu G, Patron L, Carp O, Stanica N (2003) Thermal behaviour of some iron(III) complexes with active therapeutically biguanides. J Therm Anal Calorim 72(2):489–495
6. Olar R, Badea M, Cristurean E, Lazar V, Cernat R, Balotescu C (2005) Thermal behavior, spectroscopic and biological characterization of co(II), Zn(II), Pd(II) and Pt(II) complexes with N,N-dimethylbiguanide. J Therm Anal Calorim 80(2):451–455
7. Al-Saif FA, Refat MS (2013) Synthesis, spectroscopic, and thermal investigation of transition and non-transition complexes of metformin as potential insulin-mimetic agents. J Therm Anal Calorim 111: 2079–2096
8. El-Megharbel SM (2015) Synthesis, Characterization and Antidiabetic Activity of Chromium (III) Metformin Complex. J Microb Biochem Technol 7:65–75
9. Gao JA (2007) A weak hydrolytical copper(II) complex derived from condensation of N,N-Dimethylbiguanide with 2-Pyridinecarbaldehyde synthesis, crystal structure and biological activity. Synth React Inorg Met-Org Nano-Met Chem 37(8):621–625
10. Olar R, Badea M, Marinescu D, Iorgulescu E, Stoleriu S (2005) Ni(II) complexes with ligands resulted in condensation of N,N-dimethylbiguanide and pentane-2,4-dione. J Therm Anal Calorim 80:363–367
11. Mahmoud MA, Zaitone SA, Ammar AM, Sallam SA (2006) Structure and antidiabetic activity of chromium(III) complexes of metformin Schiff-bases. J Mol Struct 1108:60–70
12. Mahmoud MA, Zaitone SA, Ammar AM, Sallam SA (2017) Synthesis, spectral, thermal and insulin enhancing properties of oxovanadium(IV) complexes of metformin Schiff-bases. J Therm Anal Calorim 128:957–969
13. Mahmoud MA, Ammar AA, Sallam SA (2017) Synthesis, characterization and toxicity of cu(II) complexes with metformin Schiff-bases. J Chin Adv Mat Soc 5:75–102

14. Taha ZA, Ajlouni AM, Al-Hassan KA, Hijazi AK, Faiq AB (2011) Syntheses, characterization, biological activity and fluorescence properties of bis-(salicylaldehyde)-1,3-propylenediimine Schiff base ligand and its lanthanide complexes. Spectrochim Acta A81: 317–323
15. Kapoor P, Fahmi N, Singh RV (2011) Microwave assisted synthesis, spectroscopic, electrochemical and DNA cleavage studies of lanthanide(III) complexes with coumarin based imines. Spectrochim Acta A83:74–81
16. Kostova I, Manolov I, Momekov G (2004) Cytotoxic activity of new neodymium (III) complexes of bis-coumarins. Eur J Med Chem 39:765–775
17. Łyszczek R (2012) Hydrothermal synthesis, thermal and luminescent investigations of lanthanide(III) coordination polymers based on the 4,4′-oxybis(benzoate) ligand. J Therm Anal Calorim 108: 1101–1110
18. Yi-Bo Z, Yang N, Liu W-S, Tang N (2003) Synthesis, characterization and DNA-binding properties of La(III) complex of chrysin. J Inorg Biochem 97:258–264
19. Wang ZM, Lin HK, Zhu SR, Liu TF, Zhou ZF, Chen YT (2000) Synthesis, characterization and cytotoxicity of lanthanum(III) complexes with novel 1,10-phenanthroline-2,9-bis-[agr]-amino acid conjugates. Anticancer Drug Des 15:405–411
20. Aime S, Crich SG, Gianolio E, Giovenzana GB, Tei L, Terreno E (2000) High sensitivity lanthanide(III) based probes for MR-medical imaging. Coord Chem Rev 250:1562–1597
21. Figgis NB, Lewis J (1960) In: Lewis J, Wilkins RG (eds) The Magnetochemistry of complex compounds. Interscience, New York
22. Geary WJ (1971) The use of conductivity measurements in organic solvents for the characterization of coordination compounds. Coord Chem Rev 7:81–122
23. Nakamoto K (1997) Infrared and Raman spectra of inorganic and coordination compounds: applications in coordination, organometallic, and bioinorganic chemistry, 5th edn. Wiley, New York
24. Kumar DS, Alexander V (1995) Macrocyclic complexes of lanthanides in identical ligand frameworks part 1. Synthesis of lanthanide(III) and yttrium(III) complexes of an 18-membered dioxatetraaza macrocycle. Inorg Chim Acta 238:63–71
25. Ankolekar VN, Mahale VB (2000) Synthesis and Spectroscopic Investigations of Lanthanide(III) Nitrate Complexes with Ligands Obtained from 2,6-diformyl-4-methylphenol. Synth React Inorg Met-Org Chem 30:1193–1209
26. Alaudeen M, Prabhakaran CP (1996) Synthesis and characterization of iron(III) complexes of N-(2-thienylidene)-N'-isonicotinoylhydrazine, N-(2-furylidene)-N'-salicyloylhydrazine and N-(2-thienylidene)-N'-salicyloylhydrazine. Indian J Chem A35:517–519
27. Muraleedharan Nair MK, Radhakrishnan PK (1996) Synthesis and physicochemical studies of yttrium and lanthanide nitrate complexes of 1,2-(diimino-4-antipyrinyl)ethane. Proc Ind Acad Sci (Chem. Sci) 108:345–350
28. Pearson RG (1936) Hard and soft acids and bases. J Am Chem Soc 85:3533–3539
29. Carlin RL (1986) Magnetochemistry. Springer, New York
30. Tandon SP, Mehta PC (1970) Study of Some Nd^{3+} Complexes: Interelectronic Repulsion, Spin–Orbit Interaction, Bonding, and Electronic Energy Levels. J Chem Phys 52:4896–4902
31. Ambroziak K, Rozwadowski Z, Dziembowska T, Bieg B (2002) Synthesis and spectroscopic study of Schiff bases derived from *trans*-1,2-diaminocyclohexane. Deuterium isotope effect on ^{13}C chemical shift. J Mol Struct 615:109–120
32. Issa RM, Khedr AM, Rizk HF (2005) UV–vis, IR and ^{1}H NMR spectroscopic studies of some Schiff bases derivatives of 4-aminoantipyrine. Spectrochim Acta A62:621–629
33. Jørgensen CK (1957) Absorption spectra of dysprosium(III), holmium(III), and erbium(III) Aquo ions. Acta Chem Scand 11: 981–989
34. Carnall WT, Fields PR, Rajnak K (1968) Electronic energy levels in the trivalent lanthanide Aquo ions. I. Pr^{3+}, Nd^{3+}, Pm^{3+}, Sm^{3+}, Dy^{3+}, Ho^{3+}, Er^{3+}, and Tm^{3+}. J Chem Phys 49:4424–4442
35. Pandey UK, Pandey OP, Sengupta SK, Tripathi SC (1987) Syntheses and spectroscopic studies on TETRAAZA MACROCYCLIC complexes of praseodymium(iii). Polyhedron 6:1611–1617
36. Davies GM, Aarons RJ, Motson GR, Jeffery JC, Adams H, Faulkner S, Ward MD (2004) Structural and near-IR photophysical studies on ternary lanthanide complexes containing poly(pyrazolyl)borate and 1,3-diketonate ligands. Dalton trans 1136-1144; Voloshin AI, Shavaleev NM, Kazakov VB (2001) luminescence of praseodymium (III) chelates from two excited states ($^{3}P_0$ and $^{1}D_2$) and its dependence on ligand triplet state energy. J Lumin 93:199–204
37. Yan B, Zhang HJ, Zhou GL, Ni JZ (2003) Different thermal decomposition process of lanthanide complexes with N-phenylanthranilic acid in air and nitrogen atmosphere. Chem Pap 57:83–86
38. Carp O, Gingasu D, Mindru I, Patron L (2006) Thermal decomposition of some copper–iron polynuclear coordination compounds containing glycine as ligand, precursors of copper ferrite. Thermochim Acta 449:55–60
39. Nyquist RA, Kagel RO (1971) Infrared spectra of inorganic compounds. Academic Press, New York
40. Coats AW, Redfern JP (1964) Kinetic parameters from thermogravimetric data. Nature 201:68–69
41. Frost AA, Pearson RG (1961) Kinetics and mechanism. Wiley, New York
42. Wells AF (1984) Structural inorganic chemistry, 5th edn. Science Publications, Oxford
43. Steiner M-S, Duerkop A, Wolfbies OS (2011) Optical methods for sensing glucose. Chem Soc Rev 40:4805–4839
44. Alptürk O, Rusin O, Fakayode SO, Wang W, Escobedo JO, Warner IM, Crowe WE, Král V, Pruet JM, Strongin RM (2006) Lanthanide complexes as fluorescent indicators for neutral sugars and cancer biomarkers. Proc Natl Acad Sci U S A 103:9756–9760
45. Yang L, Su Y, Xu Y, Zhang S, Wu J, Zhao K (2004) Interactions between metal ions and carbohydrates: the coordination behavior of neutral erythritol to zinc and europium nitrate. J Inorg Biochem 98: 1251–1260
46. Battistini E, Mortillaro A, Aime S, Peters JA (2007) Molecular recognition of sugars by lanthanide (III) complexes of a conjugate of N, N-bis[2-[bis[2-(1, 1-dimethylethoxy)-2-oxoethyl]amino]ethyl]glycine and phenylboronic acid. Contrast Media Mol Imaging 2:163–171
47. Lu Y, Deng G, Miao F, Li Z (2003) Metal ion interactions with sugars. The crystal structure and FT-IR study of the $NdCl_3$–ribose complex. Carbohydr Res 338:2913–2919
48. Wang W, Gao X, Wang B (2002) Boronic acid-based sensors. Curr Org Chem 6:1285–1317
49. Benesi HA, Hildebrand JH (1949) A Spectrophotometric Investigation of the Interaction of Iodine with Aromatic Hydrocarbons. J Am Chem Soc 71:2703–2707
50. Springsteen G, Wang B (2002) A detailed examination of boronic acid–diol complexation. Tetrahedron 58:5291–5300
51. Sun Y, Bi S, Song D, Qiao C, Mu D, Zhang H (2008) Study on the interaction mechanism between DNA and the main active components in *Scutellaria baicalensis* Georgi. Sens Actuators B: Chem 129:799–810